J. Phys. Chem. A **2002,** *106,* 6017−6023

Solvation Dynamics in the Water Pool of Aerosol Sodium Dioctylsulfosuccinate Microemulsion: Effect of Polymer

Sobhan Sen, Partha Dutta, Dipankar Sukul, and Kankan Bhattacharyya*

Physical Chemistry Department, Indian Association for the Cultivation of Science,
Jadavpur, Kolkata 700 032, India

Received: December 5, 2001; In Final Form: March 13, 2002

Solvation dynamics of 2,6-*p*-toluidinonaphthalene sulfonate (TNS) is studied in a large water pool ($w_0 = 56$) of aerosol sodium dioctylsulfosuccinate (AOT) microemulsion in *n*-heptane in the absence and the presence of a hydrophilic polymer, poly(vinylpyrrolidone) (PVP). The solvation dynamics of TNS in AOT microemulsions without polymer is found to be biexponential with a major component of 300 ± 30 ps (75%) and a slow component of 500 ± 50 ps (25%) with an average solvation time of 350 ps. In the presence of a polymer (0.75 wt % PVP) in the water pool, the solvation dynamics of TNS is found to be faster with components 70 ± 10 ps (75%) and 250 ± 25 ps (25%) and having an average solvation time of 115 ps. The very fast solvation dynamics in the presence of 0.75 wt % PVP in the water pool is similar to that in bulk water and is ascribed to strong binding of TNS to PVP. When the concentration of the polymer is increased to 2.5 wt % PVP, the solvation dynamics of TNS in polymer encapsulated microemulsions is found to be markedly slower. In the presence of 2.5 wt % PVP, the solvation dynamics in the water pool exhibits components of 100 ± 10 ps (33%), 600 ± 50 ps (47%) and 11 ± 1 ns (20%), with an average solvation time 2500 ps. This clearly indicates that, at high concentration of the polymer, dynamics of the water molecules inside the water pool of microemulsion is severely constrained.

1. Introduction

Study of water molecules in confined environments is of fundamental importance to understand how water influences the structure, dynamics, and reactivity in complex biological systems. As a result, solvation dynamics in confined environments has been the subject of many recent studies.[1−13] Among the various techniques of studying relaxation dynamics of water, ultrafast time-dependent fluorescence Stokes' shift (TDFSS) and the more recent three-photon echo peak shift (3PEPS) techniques are most suitable because of their superior time resolution down to the femtosecond time scale.[1,2] Recently, several groups have studied solvation dynamics of water in many confined environments such as cyclodextrin,[1] proteins,[3] DNA,[4] sol−gel matrix,[5] lipid vesicles,[6] water surface,[7] micelles,[8] and reverse micelles.[9,10] The most interesting feature of solvation dynamics in confined environments, is the observation of an ultraslow component, slower by 2−3 orders of magnitude compared to bulk water.[11] Several theoretical models[12] and computer simulations[13] have been applied to explain the slow component of solvation dynamics. The slow component of relaxation in confined systems is also detected in dielectric relaxation[14] and NMR studies[15] in confined environments.

A microemulsion containing a surfactant-coated nearly spherical water droplet ("water pool") is an elegant model of constrained and confined water molecules.[16] For the anionic surfactant, sodium dioctylsulfosuccinate (AOT) in a nonpolar solvent such as *n*-heptane, up to 50 water molecules per molecule of the surfactant can be trapped in the form of the water pool.[16] The radius (r_w) of the water pool is found to vary linearly with the water to surfactant mole ratio, w_0. In the case of AOT, r_w is approximately equal to $2w_0$ (in Å) in *n*-heptane.[16b]

The microemulsions have been demonstrated to be good hosts for biological and synthetic macromolecules, such as enzymes[17] and polymers.[18] There is considerable recent interest to elucidate the interaction between the polymer chains and the surfactants in the confined environment of a water pool. The interaction between a hydrophilic polymer (e.g., PVP or PEO) and an anionic surfactant (e.g., AOT or sodium dodecyl sulfate, SDS) is attractive in nature.[18,19] In bulk water, the attractive interaction between PVP (or PEO) and SDS leads to the formation of necklace-like polymer−surfactant aggregates, which consist of spherical micelles surrounded and connected by polymer strands.[19] In the water pool of a microemulsion, interaction of microemulsions with polymers has been studied by light-scattering,[18a,b] conductivity measurements,[18b,c] and Kerr effect.[18d] On addition of a water soluble polymer to the water pool, the droplet−droplet attraction is modified. In some cases, addition of polymer increases droplet−droplet attraction and, consequently, causes aggregation of the droplets. This leads to an increase in the hydrodynamic diameter.[18a,b] However, in some other cases, addition of polymer decreases droplet−droplet attraction and, hence, size.[18c,d]

There have been several studies on solvation dynamics in the water pool of microemulsions.[9−11] In the present work, we have studied how a water soluble polymer, PVP (Scheme 1a), affects droplet−droplet interaction and the solvation dynamics of water molecules in AOT microemulsions. We have chosen 2,6-*p*-toluidinonaphthalene sulfonate (TNS, Scheme 1b) as a probe. TNS, is a well-known probe for many biological systems.[20] In aqueous solution, the emission quantum yield (ϕ_f) of TNS is very small (0.001), and the lifetime (τ_f) is also very short (60 ps). With decrease in the polarity of the medium, ϕ_f and τ_f of TNS increase rapidly, and this is accompanied by a blue shift of emission maximum.[20] On binding to various

---

* To whom correspondence should be addressed. E-mail: pckb@mahendra.iacs.res.in. Fax: (91)-33-473-2805.

10.1021/jp014411t CCC: $22.00

SCHEME 1. Structure of (a) PVP and (b) TNS.

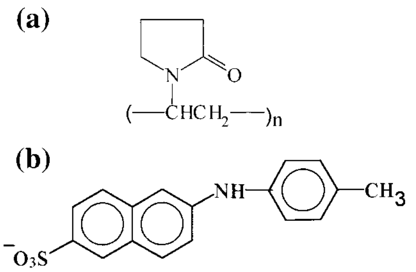

organized media, as the probe TNS is transferred from bulk water to the less-polar interior of the organized media, the emission intensity increases markedly.[20] TNS has recently been used to study solvation dynamics in many biological systems.[21] Zewail et al. detected subpicosecond components in the solvation dynamics of TNS in histone.[21a] Pierce and Boxer[21b] and Bashkin et al.,[21c] on the other hand, reported solvation dynamics of TNS in a 10 ns time scale in other proteins.

PVP is insoluble in *n*-heptane. As a result, it resides exclusively inside the water pool of the AOT reverse micelle or microemulsion. In aqueous solution, PVP remains in the cationic form and, hence, exhibits very strong affinity for the anionic species, such as TNS or AOT. We have earlier reported strong binding of TNS to PVP in aqueous solution.[23] In bulk water, addition of PVP to an aqueous solution of PVP causes a substantial increase in emission quantum yield (ϕ_f) and lifetime (τ_f) of TNS and also a marked blue shift. The ϕ_f of TNS in aqueous solution increases from 0.001 in 0 wt % PVP to 0.21 in 0.75 wt % PVP.[23] This suggests that the polarity of the microenvironment of PVP is quite low.

2. Experimental Section

2,6-*p*-Toluidinonaphthalene sulfonate, sodium salt of TNS (Sigma), is purified by repeated recrystallization from methanol−water mixture. Poly(vinylpyrrolidone) (PVP, M_w = 29 000 Da, Aldrich) and aerosol-OT (AOT, dioctylsulfosuccinate, sodium salt, Aldrich) were used as received. Preparation of the AOT microemulsion is described elsewhere.[9] The steady-state absorption and emission spectra were recorded in a JASCO 7850 spectrophotometer and a Perkin-Elmer 44B spectrofluorimeter, respectively. The extinction coefficient of TNS at 300 nm is 17 300 M^{-1} cm^{-1}. All measurements were done at 25 °C.

For lifetime measurements, the sample was excited at 300 nm by the second harmonic of a rhodamine 6G dual jet dye laser with 3,3'-diethyloxadicarbocyanine iodide (DODCI) as saturable absorber (Coherent 702-1) synchronously pumped by a CW mode-locked Nd:YAG laser (Coherent Antares 76s). The emission was collected at magic angle polarization using a Hamamatsu MCP photomultiplier (2809U). Our time-correlated single-photon-counting (TCSPC) setup consists of an Ortec 935 QUAD CFD and a Tennelec TC 863 TAC. The data are collected with a PCA3 card (Oxford) as a multichannel analyzer. The typical fwhm of the system response is about 50 ps.

The hydrodynamic radius (r) of the polymer PVP in bulk water is related to the translational diffusion coefficient (D) as, $D = kT/(6\pi\eta r)$. The diffusion measurements of the translational coefficient (D) of PVP in aqueous solutions were done in a Bruker DRX-500 NMR spectrometer, using a stimulated echo-based pulse sequence [90°−gradient pulse−90°−delay for diffusion−90°−gradient pulse acquisition].[24] The value of D is given by

$$I = \exp-[(\gamma G\delta)^2 D(\Delta - \delta/3)]$$

where I is the intensity of NMR signal, γ is the gyrromagnetic ratio, δ and Δ are delays of 2200 μs and 250 ms, respectively, in the present case, and G is the field strength. D is obtained from the slope of the plot of $-\ln(I)$ vs G^2. For 0.75 wt % aqueous PVP solution, D is found to be 1.89×10^{-6} cm^2/sec, and for 2.5 wt % aqueous PVP solution, D is 1.53×10^{-6} cm^2/sec. From this, the hydrodynamic radius (r) of PVP in bulk water is calculated to be 1.3 nm for 0.75 wt % aqueous PVP solution and 1.6 nm for 2.5 wt % aqueous PVP solution.

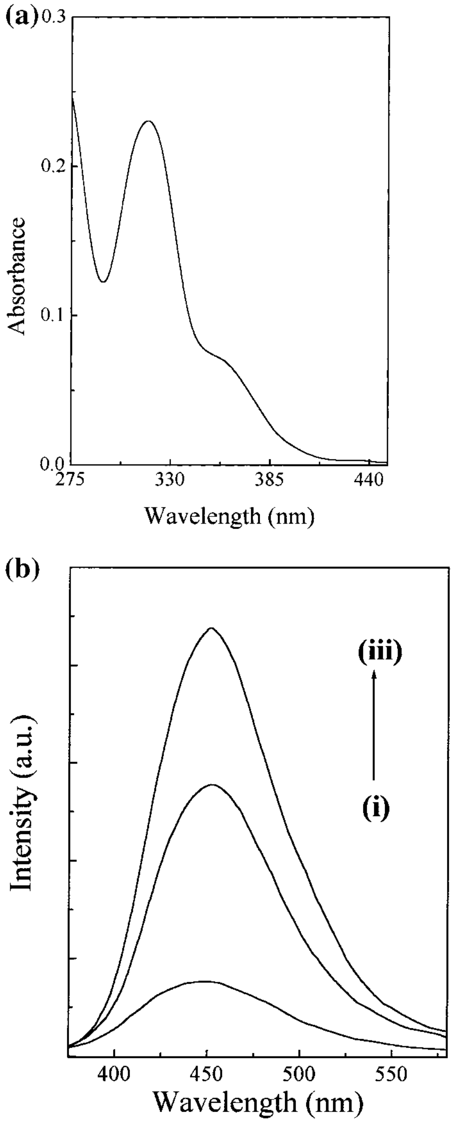

Figure 1. Absorption spectrum (a) of TNS in 90 mM AOT (w_0 = 56) in the presence of 2.5 wt % PVP and (b) steady-state emission spectra (λ_{ex} = 315 nm) of TNS in 90 mM AOT (w_0 = 56) in *n*-heptane in the presence of (i) 0, (ii) 0.75, and (iii) 2.5 wt % PVP.

Dynamic light scattering (DLS) data were recorded in a DLS-700 instrument (Otsuka Electronics Co. Ltd., Japan) fitted with a 5 mW He−Ne laser, operating at 632.8 nm, by placing the sample tube in the thermostated chamber of the goniometer. All measurements were taken at 90°. The DLS intensity data were processed using the instrumental software to obtain the hydrodynamic diameter, the polydispersity index, and the diffusion coefficient of the samples.

3. Results

3.1. Steady-State Spectra. Figure 1a shows the absorption spectrum of TNS in 90 mM AOT/*n*-heptane/water microemul-

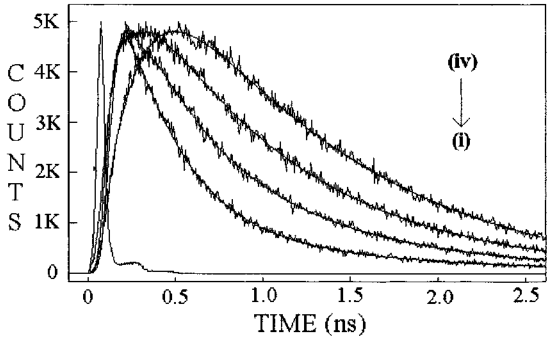

Figure 2. Fluorescence decays of TNS in 90 mM AOT/*n*-heptane/water microemulsion in the absence of PVP at (i) 390, (ii) 420, (iii) 450, and (iv) 530 nm.

sion containing 2.5 wt % PVP. The absorption spectrum is found to be identical to those of TNS in pure water or in AOT microemulsion containing 0 wt % and 0.75 wt % PVP.

Figure 1b shows the emission spectra of TNS in the water pool of AOT microemulsions at various PVP concentrations. In a small water pool (at $w_0 = 4$) within an AOT microemulsion in *n*-heptane, the emission quantum yield (ϕ_f) of TNS is 0.14, which is nearly 140 times that in water, and the emission maximum is at 440 nm, which is blue-shifted by 25 nm from that in water.[20f] With increase in w_0, as the size and polarity of the water pool increases, emission quantum yield of TNS decreases and emission maximum shows a red shift.[20e,f] At $w_0 = 56$, the emission maximum of TNS shifts to 445 nm and ϕ_f decreases to 0.03.

At $w_0 = 56$, addition of PVP to the microemulsion causes a marked increase in ϕ_f of TNS. In the water pool of $w_0 = 56$, ϕ_f of TNS rises from 0.03 in 0 wt % PVP to 0.09 for 0.75 wt % PVP and to 0.14 for 2.5 wt % PVP. At 25 °C and $w_0 = 56$, at a PVP concentration higher than 2.5 wt %, the system becomes thermodynamically unstable and the solution becomes turbid.

3.2. Time-Resolved Studies. *3.2.1. Solvation Dynamics of TNS in AOT Microemulsion in the Absence of PVP.* In pure water, the lifetime of TNS is very short (60 ps). In AOT microemulsion at $w_0 = 56$, the fluorescence decays of TNS are found to be markedly dependent on the emission wavelength (Figure 2). At the blue end of the emission (e.g., at 390 nm), the fluorescence decay is found to be triexponential with three decay components of 250 ps (74%), 690 ps (20%), and 1.31 ns (6%). However, the decay at the red end (e.g., at 530 nm) is fitted using two decay components, 980 ps and 1.2 ns, and a distinct rise of 250 ps. Such a wavelength dependence clearly indicates that TNS molecules undergo solvation dynamics. Following the procedure prescribed by Fleming and Maroncelli,[2a] the time-resolved emission spectra (TRES, Figure 3) have been constructed using the parameters of best fit to the fluorescence decays and the steady-state emission spectrum. The TRES clearly show a time-dependent Stokes' shift of the emission of TNS in AOT/*n*-heptane/water microemulsion solution. The solvation dynamics is described by the decay of the solvent correlation function, $C(t)$, defined as

$$C(t) = \frac{\nu(t) - \nu(\infty)}{\nu(0) - \nu(\infty)}$$

where $\nu(0)$, $\nu(t)$, and $\nu(\infty)$ are the peak frequencies at time 0, t, and ∞, respectively. The decay of $C(t)$ for TNS in the water pool of AOT microemulsion at $w_0 = 56$ is shown in Figure 4. The decay parameters of $C(t)$ are summarized in Table 1. It is apparent that for TNS in the AOT/*n*-heptane/water system the decay of $C(t)$ is biexponential with a fast component of 300 ± 30 ps (75%) and a slow component of 500 ± 50 ps (25%). The total Stokes' shift of the TNS emission in the AOT/*n*-heptane/water system is found to be 1670 cm^{-1}. Following Fee and Maroncelli,[2d] one may calculate the amount of solvation missed in a picosecond setup. According to this method, the difference between the emission frequency at time zero ($\nu_{\text{em}}^{\text{p}}(0)$) and the

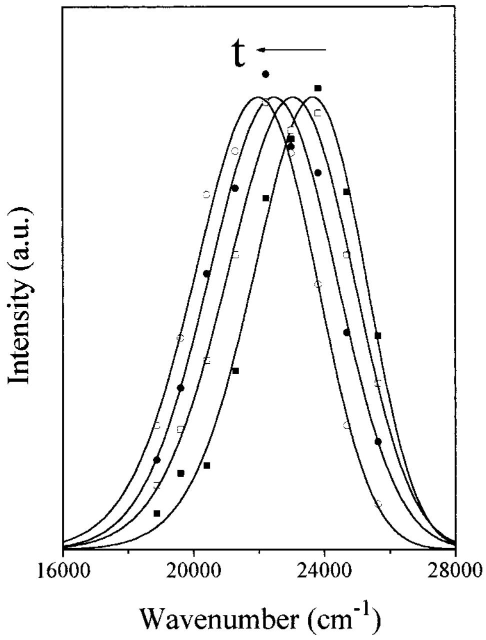

Figure 3. Time-resolved emission spectra of TNS in 90 mM AOT/*n*-heptane/water microemulsion in the absence of PVP at (■) 0, (□) 150, (●) 400, and (○) 1700 ps.

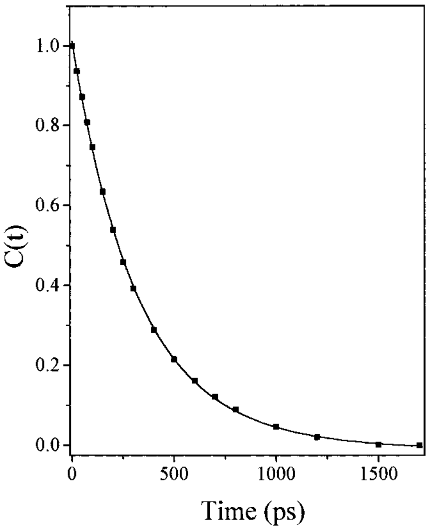

Figure 4. Decay of response function, $C(t)$, of TNS in 90 mM AOT/*n*-heptane/water microemulsion in the absence of PVP. The points denote the actual values of $C(t)$, and the solid line denotes the best fit to a biexponential decay.

TABLE 1: Decay Parameters of $C(t)$ of TNS in the 90 mM AOT/*n*-Heptane/Water System Containing 0, 0.75, and 2.5 wt % PVP

[PVP] (wt %)	$\Delta\nu$ (cm^{-1})	a_1	$\tau_1{}^a$ (ps)	a_2	$\tau_2{}^a$ (ps)	a_3	$\tau_3{}^a$ (ns)	$\langle\tau_s\rangle^{a,b}$ (ps)
0	1670	0.75	300	0.25	500			350
0.75	1560	0.75	70	0.25	250			115
2.5	1460	0.33	100	0.47	600	0.20	11	2500

[a] ±10%. [b] $\langle\tau_s\rangle = \sum a_i\tau_i$.

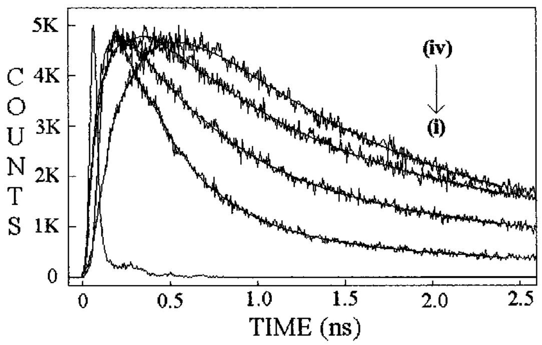

Figure 5. Fluorescence decays of TNS in 90 mM AOT/*n*-heptane/water microemulsion in the presence of 0.75 wt % PVP at (i) 390, (ii) 420, (iii) 450, and (iv) 550 nm.

absorption frequency (ν_{abs}^{p}) in a polar solvent, is approximately equal to the difference between steady-state frequencies of emission (ν_{em}^{np}) and absorption (ν_{abs}^{np}) in a nonpolar solvent. So,

$$\nu_{em}^{p}(0) = \nu_{abs}^{p} - [\nu_{abs}^{np} - \nu_{em}^{np}]$$

With the use of THF as the nonpolar solvent, $\nu_{em}^{p}(0)$ for TNS is calculated to be 24 390 cm^{-1}. From our time-resolved data for TNS in the AOT/*n*-heptane/water system, $\nu_{em}^{p}(0)$ is found to be 23 645 cm^{-1} and $\nu_{em}^{p}(\infty)$ is 21 975 cm^{-1}. Thus, in our picosecond setup, we have missed 31% of the total dynamic spectral shift. It may be recalled that even in a femtosecond setup a substantial part of the solvation is often missed. For instance, even in a femtosecond setup, Fleming et al.[2e] missed about 25% of total solvation of coumarin 343 in water.

3.2.2. Solvation Dynamics of TNS in AOT Microemulsion in the Presence of 0.75 wt % PVP. In the presence of 0.75 wt % PVP in AOT microemulsion at $w_0 = 56$, the fluorescence decays of TNS are found to be slower with significant wavelength dependence (Figure 5). In this case, at 390 nm, the decay components are 330 ps (87%) and 3.25 ns (13%). At 550 nm, two decay components of 1.40 ns and 4.65 ns and a growth component of 150 ps were observed. The TRES of TNS in the water pool of $w_0 = 56$ and in the presence of 0.75 wt % PVP are shown in Figure 6. The decay of $C(t)$ of TNS in 0.75 wt % PVP at $w_0 = 56$ is found to be biexponential with components of 70 ± 10 (75%) and 250 ± 25 ps (25%) (Figure 7). This leads to an average solvation time ($\langle\tau_s\rangle = a_1\tau_1 + a_2\tau_2$) of 115 ps. The total Stokes' shift for this case is found to be 1560 cm^{-1}. The decay parameters are summarized in the Table 1. Again from our time-resolved data, for TNS in the 0.75 wt % PVP/AOT/*n*-heptane/water system, $\nu_{em}^{p}(0)$ is 23 495 cm^{-1} and $\nu_{em}^{p}(\infty)$ is 21 935 cm^{-1}. Thus, in our picosecond setup, we have missed 36% of the total dynamic spectral shift.

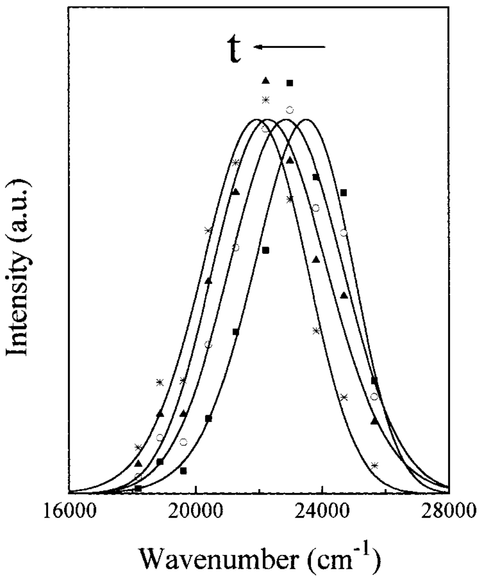

Figure 6. Time-resolved emission spectra of TNS in 90 mM AOT/*n*-heptane/water microemulsion in the presence of 0.75 wt % PVP at (■) 0, (○) 50, (▲) 150, and (∗) 800 ps.

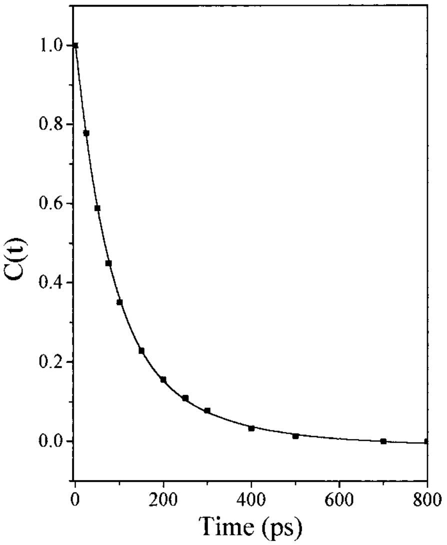

Figure 7. Decay of response function, $C(t)$, of TNS in 90 mM AOT/*n*-heptane/water microemulsion in the presence of 0.75 wt % PVP. The points denote the actual values of $C(t)$, and the solid line denotes the best fit to a biexponential decay.

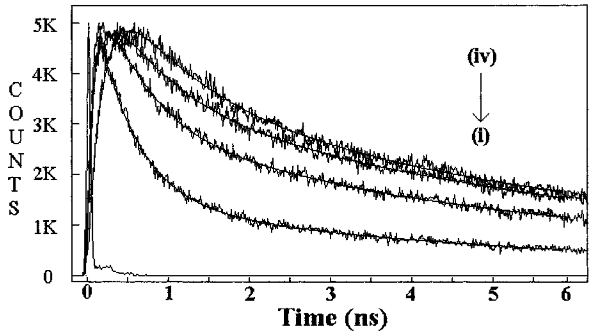

Figure 8. Fluorescence decays of TNS in 90 mM AOT/*n*-heptane/water microemulsion in the presence of 2.5 wt % PVP at (i) 395, (ii) 425, (iii) 450, and (iv) 530 nm.

3.2.3. Solvation Dynamics of TNS in AOT Microemulsion in the Presence of 2.5 wt % PVP. In the presence of 2.5 wt % PVP in AOT microemulsion at w_0 =56, the fluorescence decays of TNS are found to be slower than those in 0.75 wt % PVP with a similar and remarkable wavelength dependence (Figure 8). In this case, at 395 nm, the triexponential decay components are 150 ps (53%), 570 ps (34%), and 6.27 ns (13%). At 530 nm, two decay components, 1.10 and 8.38 ns, and a rise component of 130 ps are detected. The TRES of TNS in 2.5 wt % PVP at $w_0 = 56$ are shown in Figure 9. The decay of $C(t)$ of TNS in 2.5 wt % PVP and at $w_0 = 56$ is found to be triexponential (Figure 10) with components of 100 ± 10 ps (33%), 600 ± 50 ps (47%), and 11 ± 1 ns (20%). The average solvation time for TNS in the water pool in the presence of 2.5 wt % PVP is calculated to be 2500 ps. The total Stokes' shift in this case is 1460 cm^{-1}. The decay parameters of $C(t)$ are summarized in Table 1. From our time-resolved data, for TNS

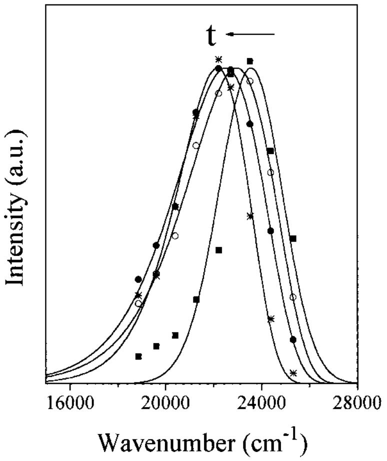

Figure 9. Time-resolved emission spectra of TNS in 90 mM AOT/*n*-heptane/water microemulsion in the presence of 2.5 wt % PVP at (■) 1, (○) 200, (●) 1000, and (*) 30 000 ps.

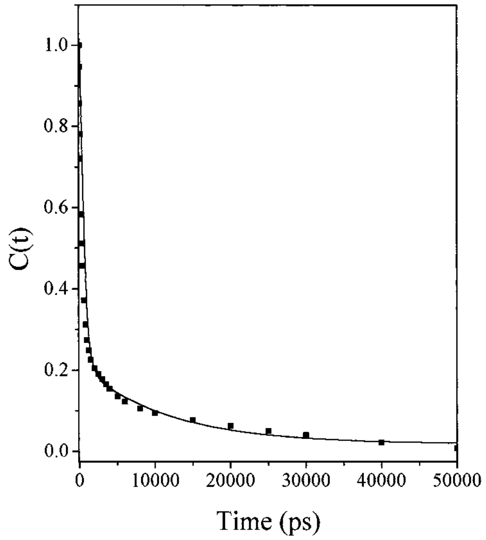

Figure 10. Decay of response function, *C*(*t*), of TNS in 90 mM AOT/*n*-heptane/water microemulsion in the presence of 2.5 wt % PVP. The points denote the actual values of *C*(*t*), and the solid line denotes the best fit to a triexponential decay.

in the 2.5 wt % PVP/AOT/*n*-heptane/water system, $\nu^{p}_{em}(0)$ is 23 575 cm^{-1} and $\nu^{p}_{em}(\infty)$ is 22 115 cm^{-1}. Thus, in our picosecond setup, we have missed 36% of the total dynamic spectral shift in the case of 2.5 wt % PVP solution in a water pool of $w_0 = 56$.

3.3 Dynamic Light Scattering. To get further insight on the effect of PVP on the AOT microemulsion, we carried out a dynamic light scattering study. Figure 11 shows the DLS data for AOT at various PVP concentrations, and Table 2 summarizes the various parameters obtained from the DLS data. It is readily seen from Figure 11 that the size distribution in all cases is unimodal. In the absence of PVP, the hydrodynamic diameter of the AOT microemulsion at $w_0 = 56$ was found to be 24 nm. In the presence of 0.75 wt % PVP in the water pool of AOT with $w_0 = 56$, there is a marked increase in the hydrodynamic diameter to 62 nm. When the PVP concentration is increased to 2.5 wt % in the water pool, the hydrodynamic diameter decreases to 31 nm.

The variation of hydrodynamic diameter of the AOT and other microemulsions on addition of water soluble polymers has been studied by several groups.[18] It is reported that addition of polymer to the water pool causes an increase in the size of the droplet in some cases[18a,b] and a decrease[18c,d] in some other cases. Brown et al.[18a,b] earlier observed nonmonotonic dependence of electrical conductivity and hydrodynamic diameter of microemulsions with increase in the concentration of a neutral polymer, PEO. They reported that the conductivity in microemulsions decreases from 0 wt % to about 1 wt % polymer and increases at higher wt %. Also, the size of the aggregates is found to increase on addition of PEO.[18b] This is ascribed to increased droplet−droplet attraction on addition of PEO.[18b] In contrast, several groups reported decrease of hydrodynamic size

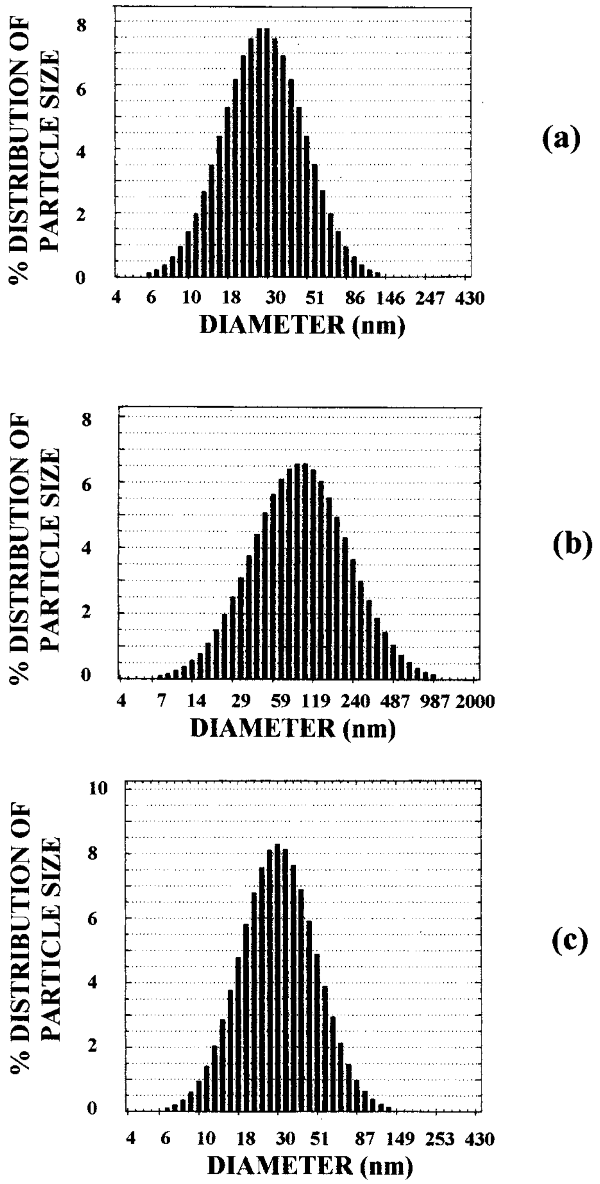

Figure 11. Dynamic light scattering data of 90 mM AOT ($w_0 = 56$) in *n*-heptane in the presence of (a) 0, (b) 0.75, and (c) 2.5 wt % PVP.

TABLE 2: Dynamic Light Scattering Data of 90 mM AOT ($w_0 = 56$) in *n*-heptane in the Presence of Different Concentrations of PVP

system (wt % PVP)	hydrodynamic diameter[a] (nm)	diffusion coefficient[a] × 10^{7} (cm^{2}/sec)	polydispersity index[b]
0	24	4.60	0.30
0.75	62	1.80	0.80
2.50	31	3.50	0.40

[a] ±10%. [b] ±0.10.

on addition of polymer, and this is attributed to reduced droplet−droplet attraction.[18c,d]

4. Discussions

The most interesting finding of this work is the marked effect of PVP on the solvation dynamics inside the water pool of AOT microemulsion and, also, the nonmonotonic dependence of hydrodynamic diameter and solvation dynamics on the PVP concentration. The hydrodynamic diameter increases from 0 (24 nm) to 0.75 wt % (62 nm) and then decreases to 31 nm as the polymer concentration increases to 2.5 wt %. The solvation dynamics, on the other hand, becomes faster as one goes from 0 wt % ($\langle\tau_s\rangle = 350$ ps) to 0.75 wt % ($\langle\tau_s\rangle = 115$ ps) and then becomes very slow at 2.5 wt % ($\langle\tau_s\rangle = 2500$ ps) PVP concentration.

The solvation time of TNS in AOT microemulsion in the absence of PVP is close to those reported earlier for other probes.[9,10] The marked increase in ϕ_f of TNS in the water pool on addition of PVP clearly indicates that TNS binds to polymer (PVP) and experiences an environment different from that in the water pool without PVP.

It should be noted that the nonmonotonic dependence of solvation dynamics in AOT microemulsion is different from that observed recently by us for PVP in aqueous solution.[23] In bulk water, average solvation time of TNS bound to PVP is 170 ps and the solvation dynamics remains unchanged as the polymer concentration increases from 0.75 to 2.5 wt %.[23]

We have noted earlier that TNS binds to PVP in the water pool as evidenced by the marked increase in ϕ_f. The observed solvation time of 115 ps for TNS in AOT microemulsion in the presence of 0.75 wt % PVP is close to the average solvation time of 170 ps for TNS bound to PVP in bulk water as reported earlier.[23] It should be noted that in the presence of 0.75 wt % PVP the size of the AOT aggregate and, hence, the water pool is about 2.6 times larger compared to the size of the water pool in the absence of PVP. The increase in the size of the water pool also may give rise to faster solvation dynamics in the presence of 0.75 wt % PVP compared to that in the absence of PVP.

The decrease in the hydrodynamic diameter of AOT aggregates from 62 nm at 0.75 wt % PVP to 31 nm at 2.5 wt % PVP indicates reduced droplet−droplet attraction at 2.5 wt % PVP. As a result of the 2-fold reduction in size and more than 3-fold increase in the concentration of PVP, the population of PVP molecules in the water pool at 2.5 wt % PVP increases more than 6 times compared with that in a water pool with 0.75 wt % PVP. This renders the movement of water molecules highly constrained inside the water pool in the case of 2.5 wt % PVP compared to the dynamics in a water pool containing 0.75 wt % PVP. For this reason, solvation dynamics becomes slower in the presence of 2.5 wt % PVP than that in the presence of 0.75 wt % PVP in AOT microemulsion.

The number of PVP molecules per water pool may be estimated as follows. From the molecular weight of PVP (29 000), 2.5 wt % PVP corresponds to 0.86 mM PVP. The aggregation number (N_{agg}) in AOT microemulsion depends on w_0. For $w_0 = 56$, N_{agg} is about 1680.[16a,b] Thus, for $w_0 = 56$, the concentration of micellar aggregates and, hence, of the water pool is 0.053 mM. If we assume the same aggregation number (N_{agg}) for AOT in the presence of 0 and 2.5 wt % PVP, there are about 16 PVP molecules per water pool in the latter. Figure 12 indicates possible locations of the TNS molecules (length ~1.4 nm) and PVP in the water pool at various PVP concentration.

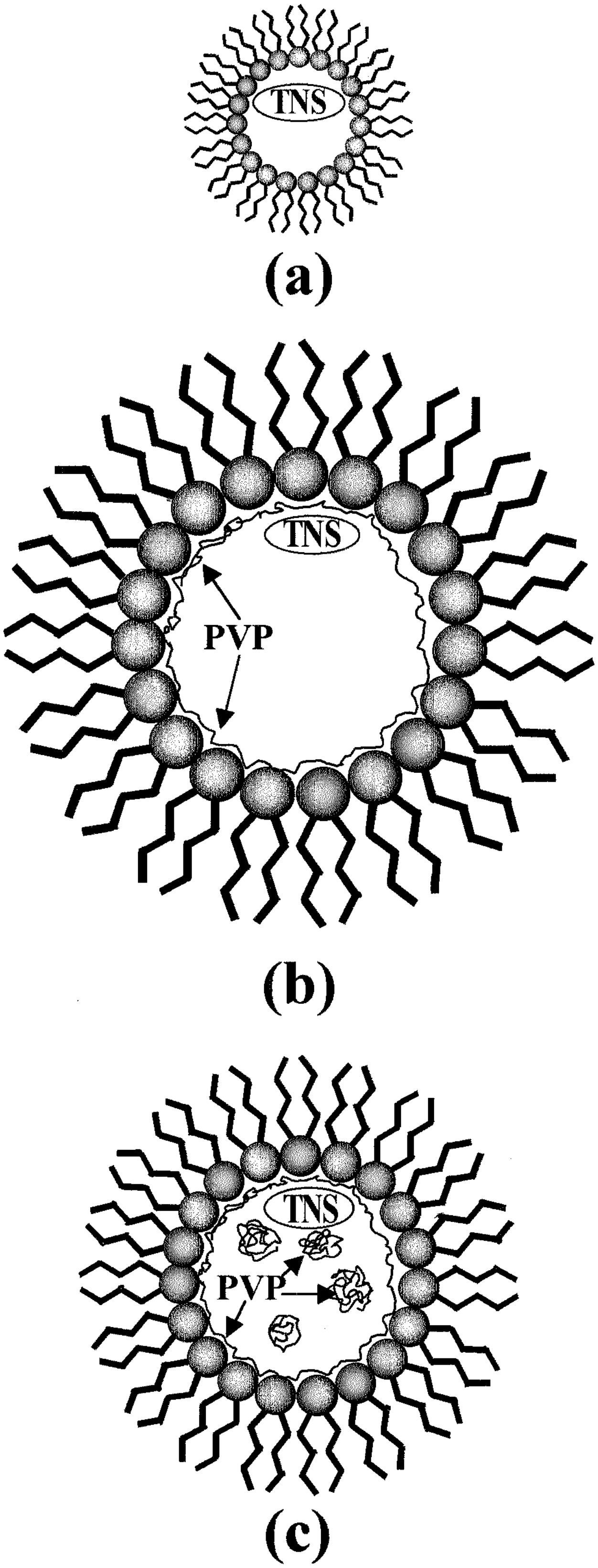

Figure 12. Schematic representation of the water pool containing (a) 0, (b) 0.75, and (c) 2.5 wt % PVP.

5. Conclusion

The present work demonstrates that both hydrodynamic diameter and solvation dynamics in the water pool of the AOT microemulsion change markedly in the presence of the polymer (PVP) and there is a nonmonotonic dependence on the concentration of PVP. In a water pool, one encounters three different situations. In the absence of the polymer, the hydrodynamic diameter is 24 nm and the average solvation time of TNS is 350 ps. At low concentration of the polymer (0.75 wt %), polymer-induced aggregation of droplets leads to the formation of large droplets of diameter 62 nm, which is about 2.6 times bigger in size compared to AOT aggregates in the absence of PVP. In this case, TNS binds very strongly with PVP in the water pool. As a result, the solvation dynamics probed by TNS is very fast with solvation time of 115 ps. The solvation time (∼115 ps) in the 0.75 wt % water pool is close to the solvation time of TNS bound to PVP in bulk water (∼170 ps), as reported earlier.[23] At a very high concentration of the polymer (2.5 wt %) in the AOT microemulsion, the hydrodynamic diameter decreases to 31 nm. The presence of about 16 polymer molecules of diameter ∼3.2 nm in each water pool severely retards the relaxation dynamics of water. As a result, in 2.5 wt % PVP, the solvation dynamics becomes very slow with an average solvation time of 2500 ps.

Acknowledgment. Thanks are due to Council of Scientific and Industrial Research (CSIR) for generous research grants. S.S., P.D., and D.S. thank CSIR for fellowships. We also thank Professor S. Roy, Bose Institute, for his help in NMR measurements and Professor S. P. Moulik for DLS measurements.

References and Notes

(1) (a) Vajda, S.; Jimenez, R.; Rosenthal, S. J.; Fidler, V.; Fleming, G. R.; Castner, E. W., Jr. *J. Chem. Soc., Faraday Trans.* **1995**, *91*, 867. (b) Nandi, N.; Bagchi, B. *J. Phys. Chem.* **1996**, *100*, 13914.

(2) (a) Maroncelli, M.; Fleming, G. R. *J. Chem. Phys*. **1987**, *86*, 6221. (b) Castner, E. W., Jr.; Maroncelli, M. *J. Mol. Liq.* **1998**, *77*, 1. (c) Stratt, R. M.; Maroncelli, M. *J. Phys. Chem.* **1996**, *100*, 12981. (d) Fee, R. S.; Maroncelli, M. *Chem. Phys.* **1994**, *183*, 235. (e) Maroncelli, M. *J. Mol. Liq.* **1993**, *57*, 1. (e) Jimenez, R.; Fleming, G. R.; Kumar, P. V.; Maroncelli, M. *Nature* **1994**, *369*, 471.

(3) (a) Jordandies, X. J.; Lang, M. J.; Song, X.; Fleming, G. R. *J. Phys. Chem. B* **1999**, *103*, 7995. (b) Homoelle, B. J.; Edington, M. D.; Diffey, W. M.; Beck, W. F. *J. Phys. Chem. B* **1998**, *102*, 3044. (c) Changenet-Barret, P.; Gooding, E. F.; Degrado, W. P.; Hochstrasser, R. M. *J. Phys. Chem. B* **2000**, *104*, 9322. (d) Pal, S. K.; Mandal, D.; Sukul, D.; Sen, S.; Bhattacharyya, K. *J. Phys. Chem. B* **2001**, *105*, 1438.

(4) Brauns, E. B.; Madaras, M. L.; Coleman, R. S.; Murphy, C. J.; Berg, M. A. *J. Am. Chem. Soc*. **1999**, *121*, 11644.

(5) (a) Pal, S. K.; Sukul, D.; Mandal, D.; Sen, S.; Bhattacharyya, K. *J. Phys. Chem. B* **2000**, *104*, 2613. (b) Loughnane, B. J.; Farrer, R. A.; Scodinu, A.; Reilly, T.; Fourkas, J. T. *J. Phys. Chem. B* **2000**, *104*, 5421.

(6) Pal, S. K.; Sukul, D.; Mandal, D.; Bhattacharyya, K. *J. Phys. Chem. B* **2000**, *104*, 4529.

(7) (a) Zimdars, D.; Dapad, J. I.; Eisenthal, K. B.; Heinz, T. F. *Chem. Phys. Lett.* **1999**, *301*, 112. (b) Benderskii, A. V.; Eisenthal, K. B. *J. Phys. Chem. B* **2000**, *104*, 11723.

(8) (a) Sarkar, N.; Datta, A.; Das, S.; Bhattacharyya, K. *J. Phys. Chem.* **1996**, *100*, 15483. (b) Pal, S. K.; Sukul, D.; Mandal, D.; Sen, S.; Bhattacharyya, K. *Chem. Phys. Lett*. **2000**, *327*, 91.

(9) (a) Pal, S. K.; Mandal, D.; Sukul, D.; Bhattacharyya, K. *Chem. Phys. Lett*. **1999**, *312*, 178. (b) Das, S.; Datta, A.; Bhattacharyya, K. *J. Phys. Chem. A* **1997**, *101*, 3299.

(10) (a) Levinger, N. E. *Curr. Opin. Colloid Interface Sci.* **2000** *5*, 118. (b) Willard, D. M.; Levinger, N. E. *J. Phys. Chem. B* **2000**, *104*, 11075. (c) Willard, D. M.; Riter, R. E.; Levinger, N. E. *J. Am. Chem. Soc.* **1998**, *120*, 4151. (d) Riter, R. E.; Undiks, E. P.; Levinger, N. E. *J. Am. Chem. Soc.* **1998**, *120*, 6062. (e) Riter, R. E.; Undiks, E. P.; Kimmel, J. R.; Pant, D. D.; Levinger, N. E. *J. Phys. Chem. B* **1998**, *102*, 7931. (f) Shirota, H.; Horie, K. *J. Phys. Chem. B* **1999**, *103*, 1437.

(11) (a) Nandi, N.; Bhattacharyya, K.; Bagchi, B. *Chem. Rev.* **2000**, *100*, 2013. (b) Bhattacharyya, K.; Bagchi, B. *J. Phys. Chem. A* **2000**, *104*, 10603.

(12) (a) Nandi, N.; Bagchi, B. *J. Phys. Chem. B* **1997**, *101*, 10954. (b) Nandi, N.; Bagchi, B. *J. Phys. Chem. A* **1998**, *102*, 8217.

(13) (a) Michael, D.; Benjamin, I. *J. Chem. Phys*. **2001**, *114*, 2817. (b) Senapathy, S.; Chandra, S. *J. Chem. Phys.* **1999**, *111*, 207. (c) Faeder, J.; Ladanyi, B. M. *J. Phys. Chem. B* **2000**, *104*, 1033. (d) Balasubramanian, S.; Bagchi, B. *J. Phys. Chem.*, in press.

(14) (a) Mashimo, S.; Kuwabara, S.; Yagihara, S.; Higasi, K. *J. Phys. Chem.* **1987**, *91*, 6337. (b) Fukuzaki, M.; Miura, N.; Sinyashiki, N.; Kunita, D.; Shiyoya, S.; Haida, M.; Mashimo, S. *J. Phys. Chem.* **1995**, *99*, 431. (c) Belton, P. S. *J. Phys. Chem*. **1995**, *99*, 17061.

(15) (a) Halle, B. In *Hydration Processes in Biology: Theoretical and Experimental Approaches*; Bellissent-Funnel, M.-C., Ed.; IOS press: Amsterdam, 1999; pp 233−249. (b) Denisov, V. P.; Halle, B. *Faraday Discuss.* **1996**, *103*, 227. (c) Otting, G.; Liepinsh, E. *Acc. Chem. Res.* **1995**, *28*, 171.

(16) (a) Cho, C. H.; Chung, M.; Lee, J.; Nguyen, T.; Singh, S.; Vedamuthu, M.; Yao, S.; Zhu, S.-B.; Robinson, G. W. *J. Phys. Chem.* **1995**, *99*, 7806. (b) Maitra, A. *J. Phys. Chem.* **1984**, *88*, 8, 5122. (c) Amararene, A.; Gindre, M.; Le Huerou, J.-Y.; Nicot, C.; Urbach, W.; Waks, M. *J. Phys. Chem. B* **1997**, *101*, 10751. (d) Moulik, S. P.; Pal, B. K. *Adv. Colloid Interface Sci.* **1998**, *78*, 99. (e) De, T.; Maitra, A. *Adv. Colloid Interface Sci.* **1995**, *59*, 95.

(17) (a) Huruguen, J. P.; Authier, M.; Greffe, J. L.; Pileni, M. P. *Langmuir* **1991**, *7*, 243. (b) Cassin, G.; Duda, Y.; Holovko, M.; Badiali, J. P.; Pileni, M. P. *J. Phys. Chem.* **1997**, *107*, 22683. (c) Avramiotis, S.; Stamatis, H.; Kolisis, F. N.; Lianos, P.; Xenakis, A. *Langmuir* **1996**, *12*, 6320.

(18) (a) Laia, C. A. T.; Brown, W.; Almgren, M.; Costa, S. M. B. *Langmuir* **2000**, *16*, 465. (b) Papoutsi, D.; Lianos, P.; Brown, W. *Langmuir* **1994**, *10*, 3402. (c) Meier, W. *J. Phys. Chem. B* **1997**, *101*, 919. (d) Suarez, M.-J.; Levy, H.; Lang, J. *J. Phys. Chem*. **1993**, *97*, 9808.

(19) (a) Norrenberg, R.; Klinger, J.; Horn, D. *Angew. Chem., Int. Ed.* **1999**, *38*, 1626. (b) Blokhus, A. M.; Klokk, K. *J. Colloid Interface Sci.* **2000**, *230*, 448. (c) Sukul, D.; Pal, S. K.; Mandal, D.; Sen, S.; Bhattacharyya, K. *J. Phys. Chem. B* **2000**, *104*, 6128. (d) Sen, S.; Sukul, D.; Dutta, P.; Bhattacharyya, K. *J. Phys. Chem. A* **2001**, *105*, 7495.

(20) (a) McClure, W. O.; Edelman, L. M. *Biochemistry* **1966**, *5*, 1908. (b) Macgregor, R. B.; Weber, G. *Nature* **1986**, *319*, 70. (c) Chang, L.; Cheung, H. C. *Chem. Phys. Lett.* **1990**, *173*, 343. (d) Das, K.; Sarkar, N.; Nath, D.; Bhattacharyya, K. *Spectrochim. Acta, Part A* **1992**, *48*, 1701. (e) Datta, A.; Mandal, D.; Pal, S. K.; Bhattacharyya, K. *J. Phys. Chem. B* **1997**, *101*, 10221. (f) Mandal, D.; Pal, S. K.; Datta, A.; Bhattacharyya, K. *Anal. Sci.* **1998**, *14*, 199.

(21) (a) Zhong, D.; Pal, S. K.; Zewail, A. H. *ChemPhysChem* **2001**, *2*, 219. (b) Pierce, D. W.; Boxer, S. G. *J. Phys. Chem.* **1992**, *96*, 5560. (c) Bashkin, J. S.; Mcledon, G.; Mukamel, S.; Marohn, J. *J. Phys. Chem.* **1990**, *94*, 4757.

(22) Maeda, Y.; Tsukida, N.; Kitano, H.; Terada, T.; Yamanaka, J. *J. Phys. Chem.* **1993**, *97*, 13903.

(23) Sen, S.; Sukul, D.; Dutta, P.; Bhattacharyya, K. *J. Phys. Chem. B* **2002**, *106*, 3763.

(24) (a) Chari, K.; Antalek, B.; Minter, J. *Phys. Rev. Lett.* **1995**, *74*, 3624. (b) Stejskal, E. O.; Tanner, J. E. *J. Chem. Phys.* **1965**, *42*, 288. (c) Cantor, C. C.; Schimmel, P. *Biophysical Chemistry*; W. H. Freeman: New York, 1980. (d) Pal, D.; Mahapatra, P; Manna, T.; Chakrabarti, P.; Bhattacharyya, B.; Banerjee, A.; Basu, G.; Roy, S. *Biochemistry* **2001**, *40*, 15512.